

Fig. 1 Typical switching function prior to balancing.

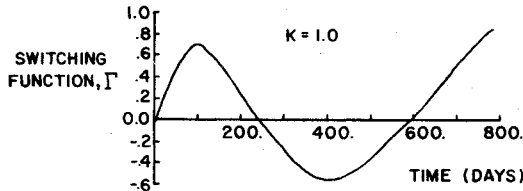
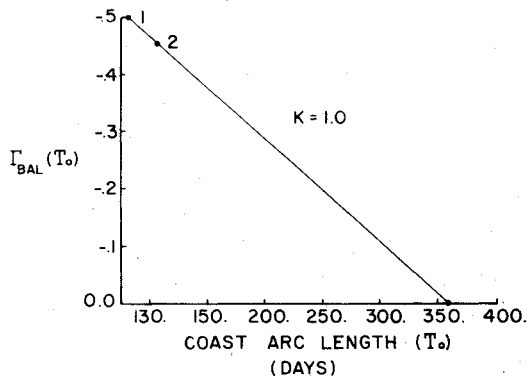
Fig. 2  $\Gamma_{BAL}$  vs  $T_0$  plot used to find optimal coast arc length.

Fig. 3 Converged switching function.

heliocentric nonrotating rectangular Cartesian coordinates,  $x_4, x_5, x_6$  are the vehicle's position components,  $u_3$  is the absolute value of the mass flow rate of the engine with  $u_3 = 0$  or  $\beta$  and  $u_1, u_2$ , are the control angles which define the thrust direction.

The performance index used was a linear combination of flight time and propellant mass expended. Previous experience with low thrust Earth-Jupiter trajectories has shown that a performance index based entirely on propellant mass often leads to very large flight times if coast arcs are allowed. Trajectories which minimize flight time result in no coast arcs. The performance index used is given by

$$J = -x_7(t_f) + K\beta t_f \quad (2)$$

The necessary conditions for minimization of the performance index subject to the equations of motion and the initial and terminal constraints are given by

$$\dot{\bar{x}} = \frac{\partial H^T}{\partial \lambda}, \quad \dot{\bar{\lambda}} = -\frac{\partial H^T}{\partial \bar{x}} = 0, \quad \frac{\partial H^T}{\partial \bar{u}} = 0 \quad (3a)$$

$$\bar{\lambda}(t_f) = \frac{\partial R^T}{\partial \bar{x}(t_f)} = \left\{ \frac{\bar{v}}{-1} \right\} \quad (3b)$$

$$\bar{M}(t_f) = \bar{0} \left( H + \frac{\partial R}{\partial t_f} \right) \Big|_{t_f} = 0 \quad (3c)$$

where the time of flight,  $t_f$ , is unspecified while  $t_0$  is fixed. The variational Hamiltonian,  $H$ , is defined in the standard manner, and  $R$  is given by

$$R = -x_7(t_f) + K\beta t_f - \bar{v}^T \bar{M}$$

where  $\bar{M}$  is the vector of terminal constraints and  $\bar{v}$  is a vector of unknown constant multipliers. The  $\bar{\lambda}$  vector is the usual time dependent Lagrange multiplier vector.

Eliminating the control in the usual fashion, using Eq. (3c) plus the requirement that  $\partial^2 H / \partial \bar{u}^2$  be positive semi-definite, we get

$$\begin{aligned} \cos u_1 &= \delta / \Delta & \sin u_1 &= -\lambda_3 / \Delta \\ \cos u_2 &= -\lambda_1 / \delta & \sin u_2 &= -\lambda_2 / \delta \end{aligned}$$

$$u_3 = \begin{cases} \beta & \text{for engine on} \\ 0 & \text{for engine off} \end{cases} \quad (4c)$$

where

$$\delta = (\lambda^2 + \lambda_2^2)^{1/2}, \quad \Delta = (\lambda_2^2 + \lambda_3^2)^{1/2} \quad \text{and} \quad \Gamma = \lambda_7 + \frac{c\Delta}{x_7} \quad (5)$$

As was stated earlier, the switching function  $\Gamma$  defined above was not used to determine coast arc entry and exit times during the iteration process, but it was used in the determination of the optimal coast arc length.

Optimal trajectories were obtained for several values of the weighting parameter  $K$ , in Eq. (2). One trajectory, with  $K = 15.0$ , exhibited no coast arc. The  $\Gamma_{BAL}$  vs  $T_0$  curve for the case  $K = 1.0$  is shown in Fig. 2. Note that the two values chosen for  $T_0$  were around 140 and 160 days while the optimal coast arc was about 350 days. The switching function for the  $K = 1.0$  case is shown in Fig. 3.

### Conclusion

An unexpected relation between coast arc length and switching function value during optimization has been found. A balancing procedure used on the switching function led to the discovery of a linear relation between the guessed coast arc length and the balanced switching function value. Through extrapolation, the optimal value of the coast arc can be precisely determined. The result is limited at present to cases where the number of switchings is two or fewer, but extensions may be possible.

### References

- <sup>1</sup>Hestenes, M.R., "Numerical Methods of Obtaining Solutions of Fixed Endpoint Problems in the Calculus of Variations," Rand Rept., RM-102, Aug. 1949.
- <sup>2</sup>Jurovics, S.A. and McIntyre, J.E., "The Adjoint Method and Its Application to Trajectory Optimization," *ARS Journal*, Vol. 32, 1962, 1354.
- <sup>3</sup>Paiewonsky, B.H., "A Study of Time Optimal Control," Aeronautical Research Associates of Princeton, Rept. 33 (June 1961); also *Proceedings of International Symposium on Nonlinear Differential Equations and Nonlinear Mechanics*, Edited by J.P. LaSalle and S. Lefschetz Academic Press, New York, 1963, pp. 333-365.
- <sup>4</sup>Tapley, B.D. and Lewallen, J.M., "Comparison of Several Numerical Optimization Methods," *JOTA*, Vol. 1, July 1967, pp. 1-28.
- <sup>5</sup>Kenneth, P. and McGill, R., "Two-Point Boundary Value Problem Techniques," *Advances in Control Systems*, Vol. 3, Academic Press, New York, 1966.

## Roll-Rate Stabilization of a Missile Configuration with Wrap-Around Fins

Peter Daniels\* and Samuel R. Hardy†  
Naval Surface Weapons Center, Dahlgren, Va.

### Nomenclature

- $d$  = reference diameter, 1.6 in.  
 $p$  = steady-state roll rate, rad/sec

Received November 17, 1975; revision received December 22, 1975.  
Index categories: LV/M Aerodynamics; LV/M Configurational Design; LV/M Dynamics, Uncontrolled.

\*Staff Engineer.

†Aerospace Engineer.

$V$  = velocity of freestream, fps  
 $\alpha$  = total angle of attack, deg  
 $\delta_A$  = aileron tab angle, deg

### Introduction

THIS paper describes results from an initial phase of a research program to determine the potential of wrap-around fins as stabilizers for air-launched weapons. As a result of a previous investigation concerned with rocket flight dynamics,<sup>1</sup> it appeared that wrap-around fin configurations of proper design may avoid roll resonance and roll-yaw coupling, thus alleviating two problems plaguing current general purpose bombs. However, a problem that is characteristic of wrap-around fin missile configurations is large roll rates at high angles of attack. The elimination of large roll rates at high angles of attack is an important factor in controlling Magnus instability of air-launched weapons, particularly bombs.<sup>2-4</sup>

The purpose of this subsonic wind tunnel study was to determine if a fin modification could be found for wrap-around fin configurations that would provide roll-rate stabilization at all angles of attack.

### Wind Tunnel Tests

Free rolling tests were conducted in the 28-in. by 40-in. subsonic wind tunnel located at Edgewood Arsenal.<sup>5</sup> The test specimen consisted of a free rolling model with an ogival nose and cylindrical afterbody, sting mounted on ball bearings. The model was designed so that various fin configurations could be easily interchanged. A schematic of the basic configuration is presented in Fig. 1. Steady-state roll rates were measured for angles of attack from 0 to 90 deg.

### Discussion of Results

The basic wrap-around fin configuration was tested, and a plot of the reduced frequency ( $pd/2V$ ) vs  $\alpha$  is shown in Fig. 2.

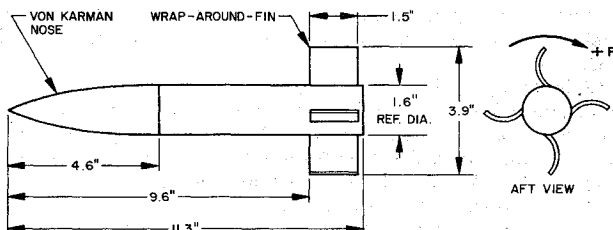


Fig. 1 Schematic of wind tunnel model (basic configuration).

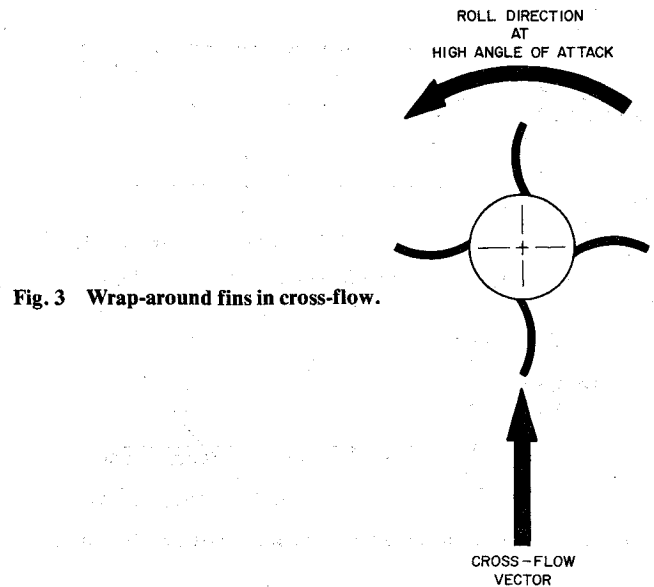


Fig. 3 Wrap-around fins in cross-flow.

This configuration exhibited large negative steady-state roll rates at high angles of attack and a small positive, steady-state roll rate at zero angle of attack. The bar indicates a region of roll lock-in, e.g., where the motion, if stopped, will remain stopped.

A straight fin configuration with the same planform as the basic wrap-around fin configuration was also tested. These test results are also presented in Fig. 2. As expected, the configuration exhibited large roll rates at high angles of attack in both the positive and negative directions.<sup>2</sup> The unsymmetrical character of the roll rates exhibited by this configuration is probably due to strut interference.

It had previously been shown that fin slots eliminated large roll rates of straight finned missiles at high angles of attack.<sup>3,4</sup> Consequently, fin slots were tested on the basic wrap-around fin configuration in the hope that the high angle of attack roll rates would be reduced. The fin slot was centrally located with an area of about 30% of the total fin area. The slot reduced the high angle-of-attack roll rates approximately 50%. Data for the slotted wrap-around fin are presented in Fig. 2.

At this point, it was obvious that an additional modification to the fin was required in order to provide roll-rate stabilization.

Since wrap-around fin configurations are not symmetrical in cross-flow as shown in Fig. 3, it was expected that a part of

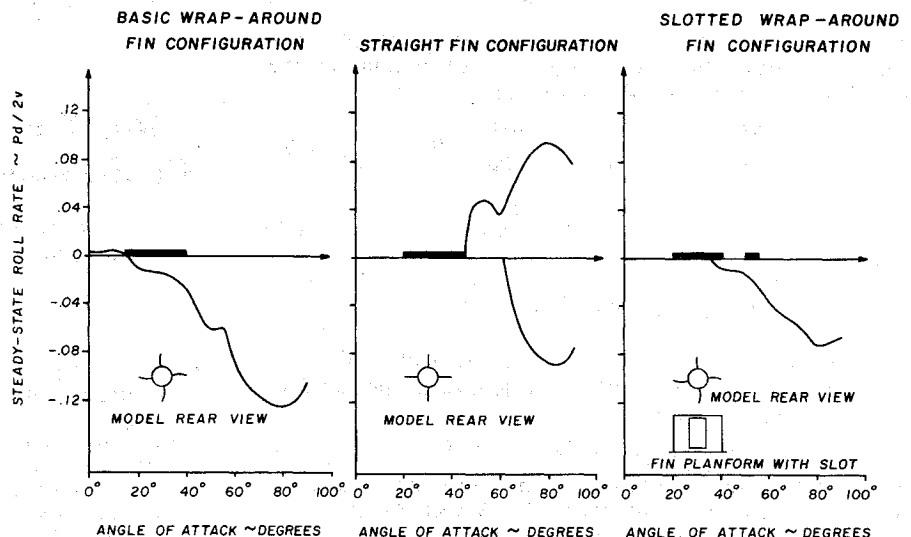


Fig. 2 Steady-state roll rate vs angle of attack.

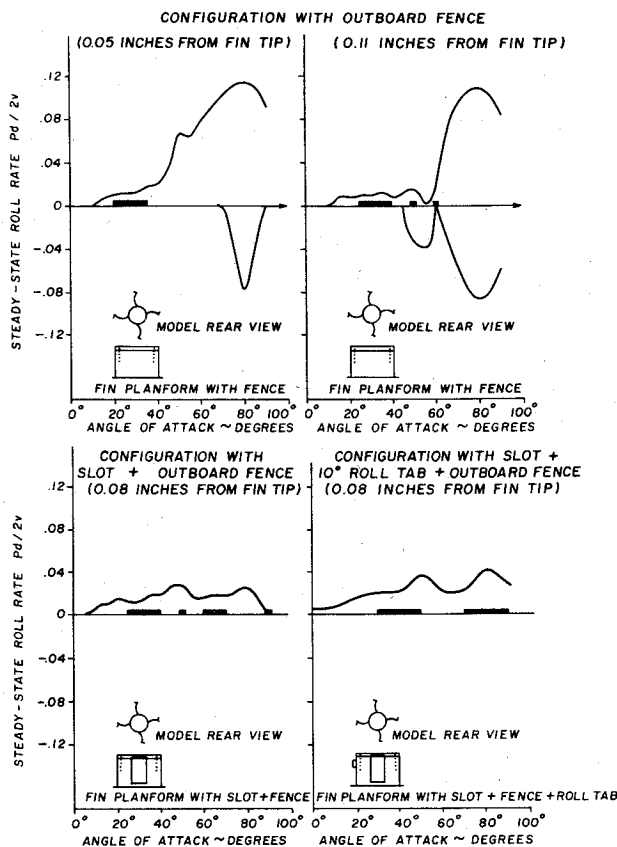


Fig. 4 Steady-state roll rate vs angle of attack for wrap-around fin configuration.

the high angle-of-attack roll rate might be produced by differential drag. Consequently, fin fences might tend to equalize the drag differential between retreating and advancing fins. Figure 4 shows the effects of fin fences on the basic wrap-around fin configuration without slots. With fences nearest the fin tip, the roll rate is reversed except at very high angles of attack where the configuration can roll in either direction. An inboard movement of the fence (0.11 in. from fin tip) gives the wrap-around fin configuration the characteristics of a straight fin configuration, e.g., the missile rolls equally well in both directions at high angles of attack.

Using a combination of slots and fences, the wrap-around configuration was then roll rate stabilized. The addition of a roll tab provided the required driving torque (see Fig. 4). The dimensions of the final roll-stabilized configuration using slots, fences, and roll tabs are given in Fig. 5. It should be noted that further refinement of the slot geometry and fence location was not attempted.

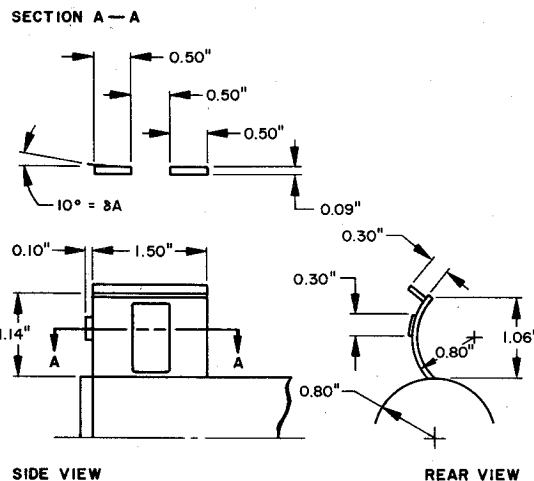


Fig. 5 Roll-stabilized wrap-around fin configuration with slot, 10° roll tab, and outboard fence 0.08 in. from fin tip.

## Conclusions

The following conclusions were made based on the results of this study: 1) missile configuration with wrap-around fins can be roll-rate stabilized using fences and slots; 2) the high angle of attack roll rates of the basic wrap-around fin configuration are probably due to vortices shed from the fins and the differential drag of the fins in cross-flow.

Surprisingly, the fence position can cause the basic wrap-around fin configuration to behave like its straight fin counterpart, probably by equalizing the drag in cross-flow. The slots eliminate the roll rates caused by vortex shedding on the wrap-around fins. Thus, the combination of fences and slots eliminates the high roll rates exhibited by wrap-around fin missile configurations at high angles of attack. The method of roll-rate stabilization presented in this report for wrap-around fin configurations is relatively simple and practical. Consequently, additional high-speed tests are strongly recommended.

## References

- Stevens, F.L., On, T.J., and Clare, T.A., "Wrap-Around vs Cruciform Fins: Effects on Rocket Flight Performance," AIAA Paper 74-777, Aug. 1974.
- Nicolaides, J.D., "Missile Flight and Astrodynamics," Bureau of Naval Weapons, Washington, D.C., TN 100-A, 1959-1961.
- Daniels, P., "A Study of the Nonlinear Rolling Motion of a Four-Finned Missile," *Journal of Spacecraft and Rockets*, Vol. 7, April 1970, pp. 510-512.
- Daniels, P., "Fin Slots vs Roll Lock-in and Roll Speed-up," *Journal of Spacecraft and Rockets*, Vol. 4, March 1967, pp. 410-412.
- Flatau, A., "Facilities and Capabilities of Aerodynamic Group Research Laboratories," Edgewood Arsenal, Edgewood, Md., EASP 100-70 of June 1970.